AMERICAN SOCIETY FOR MICROBIOLOGY | mSystems®

RESEARCH ARTICLE

Functional Insights into the Kelp Microbiome from Metagenome-Assembled Genomes

Brooke L. Weigel,[a] Khashiff K. Miranda,[b] Emily C. Fogarty,[c,d] Andrea R. Watson,[c,d] Catherine A. Pfister[e]

[a]Committee on Evolutionary Biology, University of Chicago, Chicago, Illinois, USA
[b]The College, University of Chicago, Chicago, Illinois, USA
[c]Committee on Microbiology, University of Chicago, Chicago, Illinois, USA
[d]Department of Medicine, University of Chicago, Chicago, Illinois, USA
[e]Department of Ecology & Evolution, University of Chicago, Chicago, Illinois, USA

ABSTRACT Eukaryotic organisms evolved in a microbial world and often have intimate associations with diverse bacterial groups. Kelp, brown macroalgae in the order *Laminariales*, play a vital role in coastal ecosystems, yet we know little about the functional role of the microbial symbionts that cover their photosynthetic surfaces. Here, we reconstructed 79 bacterial metagenome-assembled genomes (MAGs) from blades of the bull kelp, *Nereocystis luetkeana*, allowing us to determine their metabolic potential and functional roles. Despite the annual life history of bull kelp, nearly half of the bacterial MAGs were detected across multiple years. Diverse members of the kelp microbiome, spanning 6 bacterial phyla, contained genes for transporting and assimilating dissolved organic matter (DOM), which is secreted by kelp in large quantities and likely fuels the metabolism of these heterotrophic bacteria. Bacterial genomes also contained alginate lyase and biosynthesis genes, involved in polysaccharide degradation and biofilm formation, respectively. Kelp-associated bacterial genomes contained genes for dissimilatory nitrate reduction and urea hydrolysis, likely providing a reduced source of nitrogen to the host kelp. The genome of the most abundant member of the kelp microbiome and common macroalgal symbiont, *Granulosicoccus*, contained a full suite of genes for synthesizing cobalamin (vitamin B_{12}), suggesting that kelp-associated bacteria have the potential to provide their host kelp with vitamins. Finally, kelp-associated *Granulosicoccus* contained genes that typify the aerobic anoxygenic phototrophic bacteria, including genes for bacteriochlorophyll synthesis and photosystem II reaction center proteins, making them the first known photoheterotrophic representatives of this genus.

IMPORTANCE Kelp (brown algae in the order *Laminariales*) are foundational species that create essential habitat in temperate and arctic coastal marine ecosystems. These photosynthetic giants host millions of microbial taxa whose functions are relatively unknown, despite their potential importance for host-microbe interactions and nutrient cycling in kelp forest ecosystems. We reconstructed bacterial genomes from metagenomic samples collected from blades of the bull kelp, *Nereocystis luetkeana*, allowing us to determine the functional gene content of specific members of the kelp microbiome. These bacterial genomes spanned 6 phyla and 19 families and included common alga-associated microbial symbionts such as *Granulosicoccus*. Key functions encoded in kelp-associated bacterial genomes included dissolved organic matter assimilation, alginate metabolism, vitamin B_{12} biosynthesis, and nitrogen reduction from nitrate and urea to ammonium, potentially providing the host kelp with vitamins and reduced nitrogen.

KEYWORDS *Granulosicoccus*, alginate, dissolved organic matter, host-microbe, kelp, metagenome-assembled genomes, metagenomics, microbiome, nitrogen cycling, vitamin B_{12}

Editor Jeffrey Blanchard, University of Massachusetts Amherst

Address correspondence to Brooke L. Weigel, blweigel@uw.edu.

The authors declare no conflict of interest.

Received 24 November 2021
Accepted 13 May 2022
Published 1 June 2022

Associations between eukaryotic hosts and microbial communities are ubiquitous, yet we are just beginning to discover the functions of the microbial partners in many of these associations. Kelp, brown macroalgae in the order *Laminariales*, are among the fastest-growing and most productive marine algae (1, 2). Canopy-forming kelp species create structural habitat in temperate and arctic coastal regions worldwide (3). Photosynthetic kelp blades are covered by a dense and diverse microbiome, with up to 10^7 bacterial cells per cm^2 of kelp tissue (4, 5). Microbes associated with large habitat-forming organisms can directly influence ecosystem-level biogeochemical cycles (6), yet we know little about the functional role of the kelp microbiome.

Microbial communities associated with macroalgae are often specific to each host species and distinct from microbial communities in the surrounding seawater (7–9), yet certain bacterial groups are also shared among diverse host macroalgae (10, 11). For example, *Granulosicoccus* is an abundant bacterial symbiont on many kelps (9, 12–15), the brown alga *Fucus* (16, 17), and other diverse macroalgal hosts (18). The ubiquity of this genus points to a potentially important role, but the metabolic functions of this pervasive macroalgal symbiont are unknown.

Microbial metabolisms can greatly influence the biology of their hosts. For example, bacteria associated with phytoplankton can provide fixed or reduced nitrogen and cofactors such as vitamin B_{12} to their host algae in exchange for organic carbon (19, 20). Microbial nitrogen metabolisms such as nitrate and nitrite reduction have been identified in the microbiome of *Macrocystis pyrifera* (21), and nitrogen fixation was quantified from *M. pyrifera* blades (22). Further, the microbiome of *M. pyrifera* contained nitrite reductase genes from diverse bacterial groups, which may have increased ammonium availability to their host kelp under experimental nitrogen limitation (23). In addition to transforming nitrogen, bacteria may metabolize kelp-derived carbon. Kelp release ~16% of carbon fixed through photosynthesis into the surrounding seawater as dissolved organic carbon (DOC) (24, 25). Bacteria in the surrounding seawater consume kelp-derived DOC (26, 27), and cultured bacterial isolates from the kelp surface degrade polysaccharides such as alginate, fucoidan, laminarin, and mannitol (28, 29). However, we know little about the metabolic capabilities of kelp-associated bacterial groups in nature.

Here, we used a genome-resolved metagenomics approach to determine the functional roles and metabolic capabilities of bacterial symbionts associated with photosynthetic blades of the canopy-forming bull kelp (*Nereocystis luetkeana*). The bull kelp microbiome is comprised of a few microbial taxa that persist across geographic locations (9), colonize new tissues rapidly (30), reach high cell densities, and display repeatable micrometer-scale spatial structure (5). We reconstructed 79 bacterial metagenome-assembled genomes (MAGs) from bull kelp blade tissues, spanning 6 bacterial phyla and 19 families. By assembling bacterial genomes from kelp blades over 3 consecutive years, we tested whether the annual life history of *N. luetkeana* affects the continuity of bacterial taxa across years. We evaluated whether microbial metabolisms that are likely to interact with host kelp metabolisms or contribute to nutrient cycling in kelp forest ecosystems are present in kelp-associated bacterial genomes by searching for genes related to dissolved organic matter (DOM) assimilation, laminarin and alginate metabolism, nitrogen metabolism, and vitamin B_{12} biosynthesis. We tested the hypothesis that kelp-associated microbes have the capacity to consume dissolved organic matter (DOM) by searching for cell membrane DOM transport proteins in the assembled bacterial genomes, which are used by bacteria to assimilate DOM (31, 32). Finally, we determined the metabolic functions of the most abundant member of the kelp microbiome, *Granulosicoccus*. Pangenomic comparisons of kelp-associated *Granulosicoccus* MAGs to other available *Granulosicoccus* genomes facilitated the discovery of novel functions associated with this bacterial genus.

RESULTS

Bacterial genomes assembled from kelp blade surface swabs and whole kelp tissues. Shotgun metagenomic sequencing of 7 samples collected from blades of *N. luetkeana* resulted in 156.4 million high-quality short reads, with an average of 22 million reads

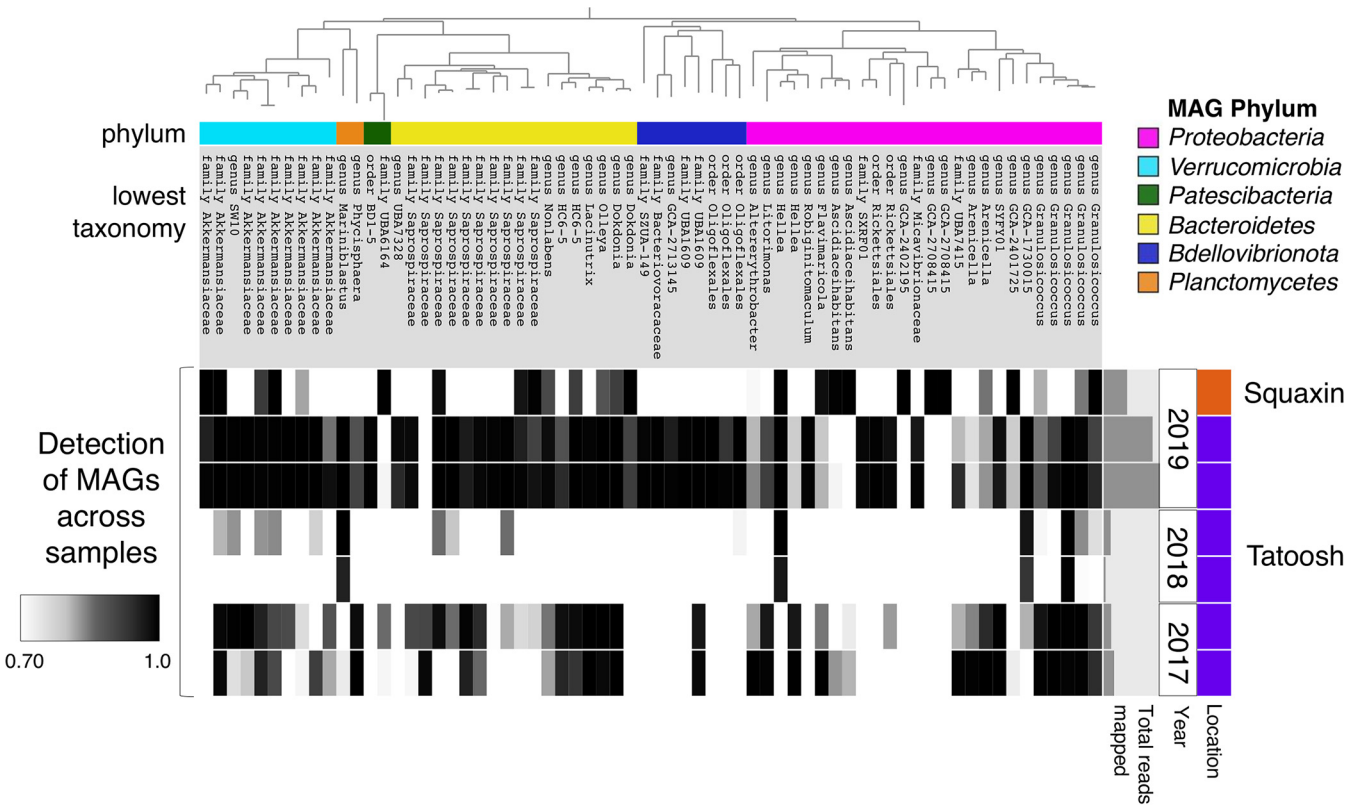

FIG 1 A maximum-likelihood phylogenetic tree of the 66 unique metagenome-assembled genomes (MAGs) (top), colored by bacterial phylum with the lowest taxonomy listed for each MAG, showing the detection of MAGs (columns) across different kelp metagenome samples (rows). MAGs are considered present in a sample if at least 70% of the genome is covered by at least one short read from that sample, so detection ranges from 0.70 to 1.0 (black and gray bars in the heatmap). White bars in the heatmap indicate the absence of a MAG in that sample, where less than 70% of the genome is covered by short reads from that sample. Samples are grouped by location and year, and the small bar graph to the right shows the total number of short reads mapped to all MAGs in each metagenome sample.

per sample (see Table S1 in the supplemental material). We manually reconstructed 79 MAGs from both whole kelp blade tissue samples and blade surface swabs. These MAGs belong to 6 different bacterial phyla, including 16 from the class *Gammaproteobacteria*, 15 from the class *Alphaproteobacteria*, 22 of *Bacteroidetes*, 13 of *Verrucomicrobia*, 9 of *Bdellovibrionota*, 2 of *Planctomycetes*, and 2 of *Patescibacteria* (Table S2 and Fig. S1). Of the 79 MAGs, 13 were redundant (>99% average nucleotide identity [ANI]), yielding a final data set of 66 unique or nonredundant MAGs (Table S2). Metagenomic assemblies from whole kelp tissue samples contained 39.0 to 49.8% kelp host DNA, so despite the mix of kelp and bacterial genomes, approximately half of the sequences were bacterial. Read recruitment of short reads from each metagenome sample to the assembled MAGs revealed that surface swabs were more effective at capturing bacterial genomes, with less host contamination. Metagenomic samples assembled from kelp surface swabs yielded a higher percentage of sequences that mapped to bacterial genomes (88.2%) than did samples assembled from kelp tissues (37.3%; Table S1). This also indicates that the MAGs captured most of the bacterial reads present in metagenomic samples.

Detection and abundance of bacterial genomes that persist over multiple years. We assembled bacterial genomes collected from *N. luetkeana* blades on Tatoosh Island in 2017, 2018, and 2019 and from Squaxin Island in 2019. Read recruitment of short reads from each metagenome to assembled bacterial genomes revealed that 31 MAGs (47% of the total number of unique MAGs) were detected (defined as >70% of the genome covered by short reads from that sample) across 2 or more years, and 15 were detected in both locations (Fig. 1). In contrast, 30 MAGs (45%) were detected in only a single year or at a single location. A single MAG of *Granulosicoccus* (g4_MAG_00004) was detected in all samples from Tatoosh Island in 2017, 2018, and 2019 (Fig. 1). However, metagenomes

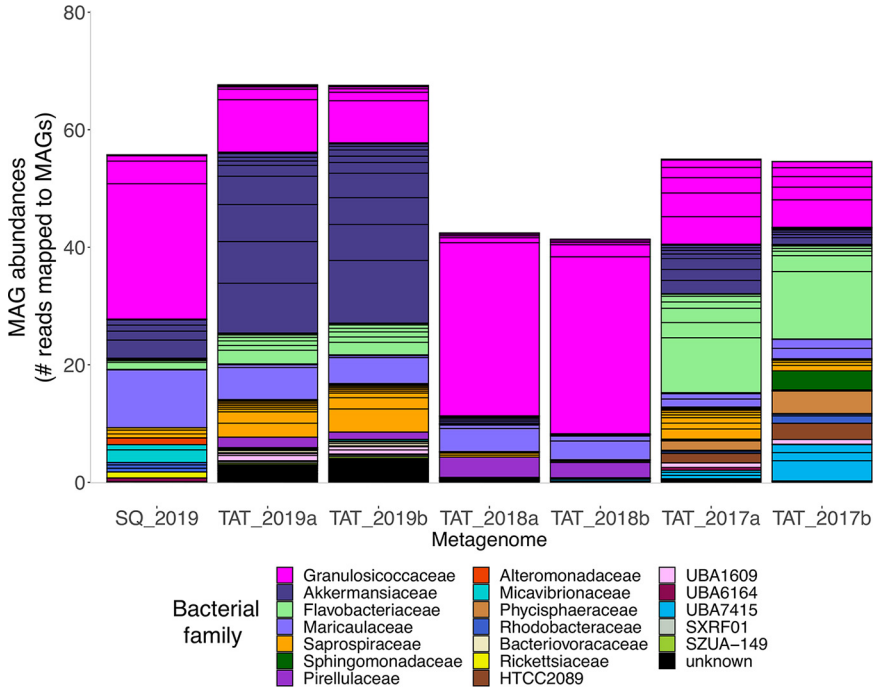

FIG 2 Abundance of kelp-associated MAGs, colored by bacterial family, within each metagenome sample. Black outlines within each colored bar indicate distinct MAGs belonging to each family. On the *x* axis, metagenomes from Tatoosh (TAT) and Squaxin (SQ) are indicated along with sampling year. Abundance is defined as the mean coverage of a MAG (number of metagenomic short reads mapped across the genome) divided by that sample's overall mean coverage. For example, an abundance value of 10 indicates that the MAG's mean coverage is 10 times that of the mean for all MAGs in that sample. See Table S3 in the supplemental material for abundance values of individual MAGs in metagenome samples.

from 2018 had a low rate of detection of bacterial MAGs (Fig. 1), likely because they were assembled from whole kelp tissues. Excluding the 2018 samples, 26 MAGs (39%) were detected in both 2017 and 2019 on Tatoosh Island.

While detection indicates the presence or absence of a MAG, abundance reveals the relative proportions of MAGs within a sample, based on the number of metagenomic short reads that mapped to each MAG. *Granulosicoccus* was the most abundant bacterial genome assembled from kelp at both locations (Fig. 2). Together, the 5 nonredundant MAGs of *Granulosicoccus* recruited an average of 40% of the total metagenomic reads across samples, with a range of 12% to 75% per sample. Different genomes of *Granulosicoccus* were differentially abundant at each location (Table S3), which are likely distinct species based on their ANI of 82% (Fig. S2). The next most abundant bacterial genomes included multiple MAGs from the family *Akkermansiaceae* (phylum *Verrucomicrobia*), *Dokdonia* (family *Flavobacteriaceae*), and *Hellea* (family *Maricaulaceae*) (Fig. 2). Together, just 8 MAGs including 4 of *Granulosicoccus*, 2 of *Akkermansiaceae*, 1 *Dokdonia*, and 1 *Hellea* accounted for 41% to 82% of all short reads mapped to kelp metagenomes (Table S3). Other abundant taxa included MAGs from the family *Saprospiraceae* (phylum *Bacteroidetes*), *Mariniblastus* (family *Pirellulaceae*), and *Lacinutrix* (family *Flavobacteriaceae*) (Fig. 2; Table S3).

Widespread occurrence of genes for DOM transport by diverse bacteria. We detected the presence of 72 genes for dissolved organic matter (DOM) assimilation among the 66 unique bacterial genomes assembled from the kelp surface (Fig. 3A; Table S4). Genes identified in kelp-associated bacterial genomes transported diverse DOM substrates, including amino acids, oligopeptides, polyamines, lipids (long-chain fatty acids and glycerol), nucleotides, carbohydrate sugars, carboxylic acids, and solutes (Fig. 3A; Table S4). DOM transport proteins were present in members of all bacterial phyla and in almost every bacterial genome, with the exception of one MAG from the

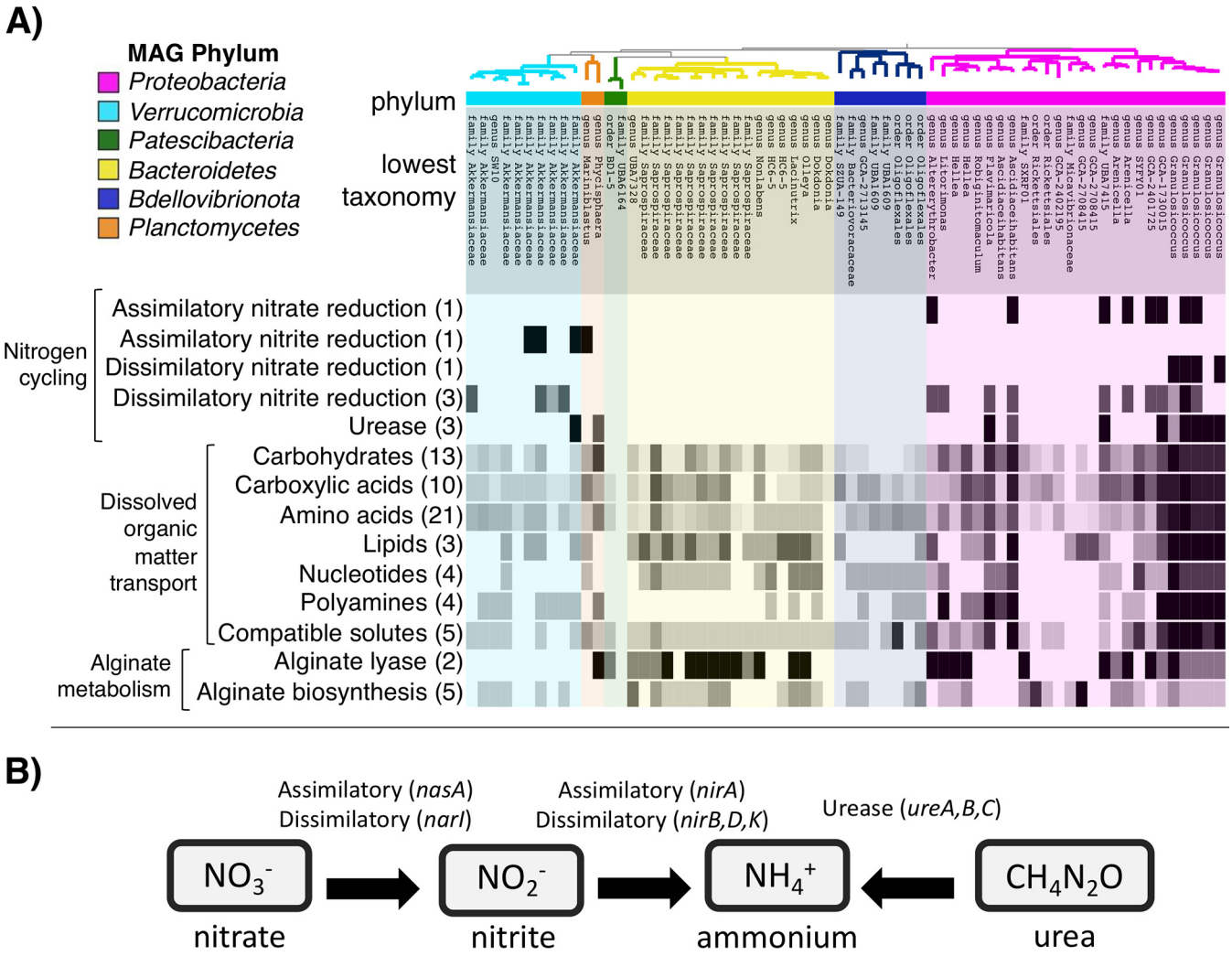

FIG 3 (A) Presence and absence of genes (rows) involved in nitrogen cycling, dissolved organic matter transport, and alginate metabolism across kelp-associated bacterial genomes (columns). The tips of the phylogeny represent the 66 unique bacterial genomes (MAGs), colored by phylum, with the lowest taxonomic level and name. The number of genes in each category is listed in parentheses to the left of the heatmap, and the shade of the heatmap indicates the number of genes present in each MAG. Dissolved organic matter transporter genes are grouped by substrate type. See Tables S4 and S5 in the supplemental material for expanded lists of DOM transport, nitrogen cycling, and alginate metabolism gene presence or absence across MAGs. (B) Diagram of the nitrogen transformation genes contained in kelp-associated bacterial genomes listed above.

phylum *Patescibacteria* and family UBA6164 (Fig. 3A). Most bacterial genomes contained multiple genes for DOM transport, with a median of 14 genes per genome (Table S4). Genomes of *Granulosicoccus* contained the highest number of DOM transporters, with a range of 53 to 59 distinct transport protein genes per genome (Fig. 3A; Table S4). Many of these genes are ATP-binding cassette (ABC)-type transporters, fueled by ATP hydrolysis to actively translocate substrates across the bacterial cell membrane (33). ABC-type transporters involved in transporting amino acids and oligopeptides and sugars such as xylose, ribose, and arabinose were present in diverse bacterial genomes (Table S4). In addition to ABC-type transporters, bacterial genomes contained genes for permeases that facilitate transport across the membrane (e.g., fucose permease), as well as tripartite ATP-independent periplasmic (TRAP)-type transporters for mannitol and carboxylic acids (Table S4).

Alginate degradation, and production, by kelp surface bacteria. Alginate lyase genes, including poly(beta-D-mannuronate) lyase (*algL*) and oligoalginate lyase (*alg17C*), were present in 4 bacterial phyla and 10 bacterial families but were most common in MAGs from the *Bacteroidetes* (family *Saprospiraceae*), *Alphaproteobacteria* (*Hellea*, *Litorimonas*, and *Altererythrobacter*), and *Gammaproteobacteria* (*Arenicella*,

families UBA7415 and *Granulosicoccaceae*) (Fig. 3A; Table S5). While some bacteria degrade alginate, others synthesize this polysaccharide as a component of extracellular biofilm formation. One *Alphaproteobacteria* member in the genus GCA-2708415 (family *Micavibrionaceae*) contained 5 alginate biosynthesis genes (Fig. 3A; Table S5). The *algE* gene, responsible for the export of synthesized alginate (34), was present in *Granulosicoccus* and the *Alphaproteobacteria* member GCA-2708415. In contrast to alginate lyase genes, genes encoding laminarinase enzymes, also known as endo-1,3-beta-D-glucosidases, were surprisingly absent from kelp-associated bacterial genomes (Table S5). Additional carbohydrate metabolism genes, likely to play a role in degradation of mucin and sulfated polysaccharides, were abundant in the genome of *Akkermansiaceae*, including 66 sulfatase genes, 3 ABC-type polysaccharide transporter genes, and 24 *N*-acetylglucosamine metabolism genes.

Nitrogen metabolisms in the kelp microbiome. Kelp-associated bacterial genomes from the *Proteobacteria*, *Verrucomicrobia*, and *Planctomycetes* contained genes for dissimilatory nitrate and nitrite reduction and urea hydrolysis (Fig. 3A and B). MAGs in the family *Akkermansiaceae* (phylum *Verrucomicrobia*) contained genes for dissimilatory nitrite reduction (*nirA*, *nirB*, and *nirD*; Table S5). One *Akkermansiaceae* member also had the ability to hydrolyze urea with genes encoding the three urease subunits (*ureABC*). The *Planctomycetes Mariniblastus* contained a gene for nitrite reduction (*nirA*), and *Phycisphaera* had *ureAB* and *ureC*. The greatest diversity of nitrogen metabolisms was found within the *Proteobacteria* (Fig. 3A; Table S5). Multiple MAGs contained both nitrate and nitrite reduction genes, indicating the potential for reduction from nitrate to ammonium, including *Altererythrobacter*, *Ascidiaceihabitans*, *Arenicella*, and *Granulosicoccus* (Fig. 3A; Table S5). *Proteobacteria* with urease genes (*ureABC*) included *Ascidiaceihabitans*, *Flavimaricola*, *Arenicella*, and *Granulosicoccus* (Fig. 3A; Table S5). *Granulosicoccus* MAGs contained genes for assimilatory and dissimilatory nitrate reduction (*nasA* and *narI*, respectively), dissimilatory nitrite reduction (*nirBDK*), and urease (Fig. 3A and B).

***Granulosicoccus* pangenome reveals high genomic diversity and diverse metabolisms.** We assembled 8 *Granulosicoccus* genomes, with an average genome length of 4,292,108 bp and an average GC content of 49.02%. *Granulosicoccus* MAGs were assembled from samples collected in all 3 years and at both locations and range in completion from 77.5 to 98.6% complete, with 6 MAGs >90% complete with <5% contamination (Table S2). The demarcation for a bacterial species using whole-genome average nucleotide identity (ANI) is typically ≥95% (35), while ANI values across genera average 73% (36). The mean ANI between *Granulosicoccus* MAGs in this study was 81.3%, but the MAGs clustered into 4 distinct clades with an ANI of >98% within each clade, likely representing 4 distinct species within the genus *Granulosicoccus* (Fig. S2). We analyzed the pangenome of these 8 *Granulosicoccus* genomes together with genomes of *Granulosicoccus antarcticus* type strain IMCC3135 (37) and *Granulosicoccus* MAG 002746645 (38). The mean ANI between MAGs in this study and the reference genomes was 71.9% for *G. antarcticus* and 70.2% for *Granulosicoccus* MAG 002746645. Two kelp-associated MAGs were more closely related to *G. antarcticus* (>72% ANI) than the others (Fig. S2).

The *Granulosicoccus* pangenome contained a core genome of 6,222 genes shared among all 10 genomes (15% of the total number of genes in the pangenome), a large accessory genome of 26,873 genes that were present in at least two but not all genomes (66% of the pangenome), and 7,684 unique genes (19%) that were present in only a single genome (Fig. S3). Genes related to amino acid, carbohydrate, and lipid transport and metabolism were among the most abundant gene clusters in the core genome (Table S6), along with essential cellular functions such as transcription, translation, and cell wall biogenesis. The core genome also contained many gene clusters related to cell motility (Table S6).

Granulosicoccus MAGs in this study contained diverse metabolic genes related to DOM transport, nitrogen and sulfur transformation, motility and chemotaxis, aerobic respiration, and cobalamin (B_{12}) synthesis (Table 1 and Fig. 4). *Granulosicoccus* contained

TABLE 1 Functional categories and metabolisms present in the *Granulosicoccus* pangenome[a]

Functional category	*G. antarcticus*	*Granulosicoccus* MAG 002746645	*Granulosicoccus* MAGs (this study)
Synthesis of bacteriochlorophyll			
Magnesium chelatase (*bchHI*)	−	−	7/8
Bacteriochlorophyllide reductase (*bchXYZ*)	−	−	7/8
Light-independent protochlorophyllide reductase (*chlLNB*)	−	−	7/8
Photosystem II			
Light-harvesting complex 1 alpha chain (*pufAB*)	−	−	7/8
Photosystem II reaction center (*pufLM*)	−	−	7/8
Photosynthetic reaction center cytochrome *c* subunit	−	−	7/8
Nitrogen metabolisms			
Nitrate reduction (NO_3 to NO_2)	+	−	4/8
Nitrite reduction (NO_2 to NH_4)	+	−	6/8
Urease (CH_4N_2O to NH_4 and CO_2)	+	−	8/8
Urea transporter	+	−	6/8
Sulfur metabolisms			
Assimilatory sulfate reduction (sulfate to hydrogen sulfide)	+	−	8/8
Thiosulfate oxidation by sox (thiosulfate to sulfate)	+	−	5/8
Sulfide oxidation	+	+	0/8
DMSP transformation	+	−	6/8
Vitamin B_{12} (cobalamin) biosynthesis			
Corrin ring biosynthesis	+	+	1/8
Cobalt insertion into corrin ring (anaerobic pathway)	−	−	1/8
Cobalt insertion into corrin ring (aerobic pathway)	+	+	8/8
Final B_{12} biosynthesis and repair	+	+	7/8
Catalyzes B_{12} into coenzyme form	+	+	8/8
B_{12} membrane transporter	+	+	7/8
Motility and chemotaxis			
Motility—flagella	+	+	8/8
Motility—type IV pilus	+	+	8/8
Chemotaxis	+	+	8/8

[a]For the genomes of *G. antarcticus* and *Granulosicoccus* MAG 002746645, presence (+) or absence (−) of each function is indicated. For the kelp-associated *Granulosicoccus* MAGs, *X*/8 indicates the number of genomes containing genes for each function out of the 8 assembled genomes.

15 genes for aerobic respiration via the citrate cycle (Fig. 4). Surprisingly, *Granulosicoccus* genomes assembled from the kelp surface contained genes for bacteriochlorophyll synthesis and photosystem II (PSII) reaction center proteins (Table 1), making them a novel clade of aerobic anoxygenic phototrophic (AAP) bacteria (detailed below). *Granulosicoccus* MAGs contained 64 different genes encoding DOM transport proteins (Fig. 4; Table S4). Similar to previously reported motility genes in *G. antarcticus* (37), all 8 MAGs contained genes for synthesizing flagella (32 genes) and type IV pili (17 genes), and they contained 11 genes related to chemotaxis (Fig. 4, Table 1, and Table S7).

Granulosicoccus MAGs contained genes to transform both nitrogen and sulfur. Genomes of *Granulosicoccus* contained dissimilatory nitrate (*narI*) and nitrite (*nirB*, *nirD*, and *nirK*) reduction genes, indicating the potential for complete dissimilatory nitrate reduction to ammonium (Fig. 3A and Table 1). *G. antarcticus* contained additional nitrate reductases (*narG*, *narY*, and *narI*) that were not present in the kelp-associated MAGs (Table S7). *G. antarcticus* and kelp-associated *Granulosicoccus* MAGs contained urease genes (*ureABC*) and urea transport proteins (Fig. 3A and Table 1). *Granulosicoccus* genomes contained sulfur metabolism genes including assimilatory sulfate reduction (*cysNC*, *cysH*, *cysI*, and *cysJ*) and *sox* genes for thiosulfate oxidation to sulfate (Table 1). Closely related bacteria in the family *Granulosicoccaceae* are capable of chemolithotrophic growth by oxidizing sulfur compounds (39), but the function of these sulfur metabolisms in kelp-associated *Granulosicoccus* has yet to be determined (37). As reported previously for *G. antarcticus* (37), kelp-associated MAGs of *Granulosicoccus* contained dimethylsulfoniopropionate (DMSP) demethylase (*dmdA*), the only enzyme known to demethylate

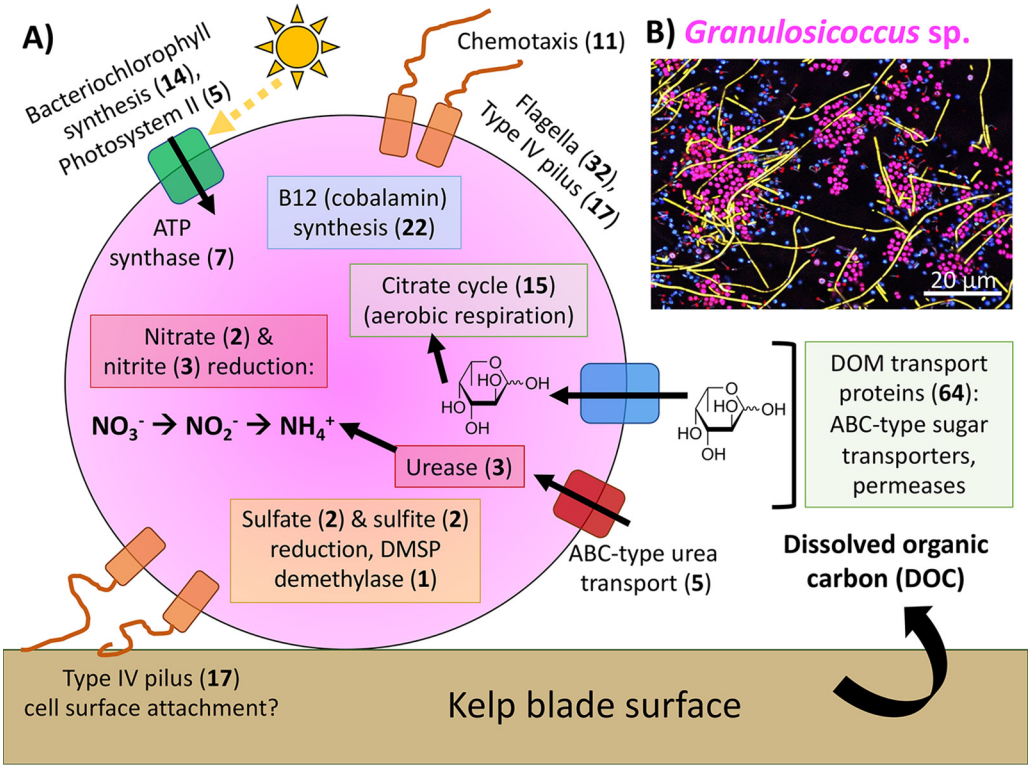

FIG 4 (A) Conceptual model of the functions and metabolisms of *Granulosicoccus* that are important to its role as a macroalgal symbiont, based on functional gene annotations of 8 MAGs assembled from bull kelp blades. Bold numbers in parentheses indicate the number of unique genes associated with each function. (B) Image of the micrometer-scale spatial structure of the *N. luetkeana* surface microbiome depicting clusters of magenta *Granulosicoccus* cells (coccus shaped), adapted with permission from the work of Ramírez-Puebla et al. (5).

DMSP (37), an organic sulfur compound produced by algae that plays a significant role in the global sulfur cycle (40).

Finally, *Granulosicoccus* MAGs contained many of the genes necessary for cobalamin (vitamin B_{12}) synthesis (Fig. 4; Table S7), a vitamin generally lacking in host macroalgae (41). While only one MAG (g3_MAG_00002) contained all 22 genes necessary for complete synthesis of B_{12}, including 11 genes involved in corrin ring synthesis, 7 out of 8 MAGs contained at least 10 genes for B_{12} biosynthesis (Table 1; Table S7). Further, all 8 MAGs contained the genes to catalyze B_{12} into its coenzyme form as well as insert cobalt into the corrin ring through the aerobic pathway (*cobS* and *cobT*), and 7 out of 8 genomes contained the B_{12} membrane transporter gene *btuB* (Table 1; Table S7). Interestingly, the MAG with a complete biosynthesis pathway contained genes for insertion of cobalt into the corrin ring through both aerobic and anerobic pathways (Table S7). Other bacterial taxa contained many of the required genes for B_{12} biosynthesis, including the *Gammaproteobacteria* UBA7415 (16 genes) and *Arenicella* (9 genes), and the *Alphaproteobacteria Ascidiaceihabitans* (11 genes) and *Flavimaricola* (14 genes).

While a full kelp genome would confirm that *N. luetkeana* requires B_{12}, we found genes for the B_{12}-dependent (cobalamin-binding) methylmalonyl coenzyme A (CoA) mutase (MCM) in the partial host kelp genomes in both samples extracted from whole kelp tissues. If the host kelp has this B_{12}-dependent enzyme, it requires vitamin B_{12} (42, 43) and may be dependent on associated bacteria for B_{12} synthesis. Using a protein BLAST search, these MCM amino acid sequences from *N. luetkeana* matched with 93% sequence identity to an unknown protein from the brown alga *Ectocarpus siliculosus* and with >80% sequence identity to B_{12}-dependent methylmalonyl-CoA mutase proteins from other closely related eukaryotes, including *Phytophthora parasitica* and

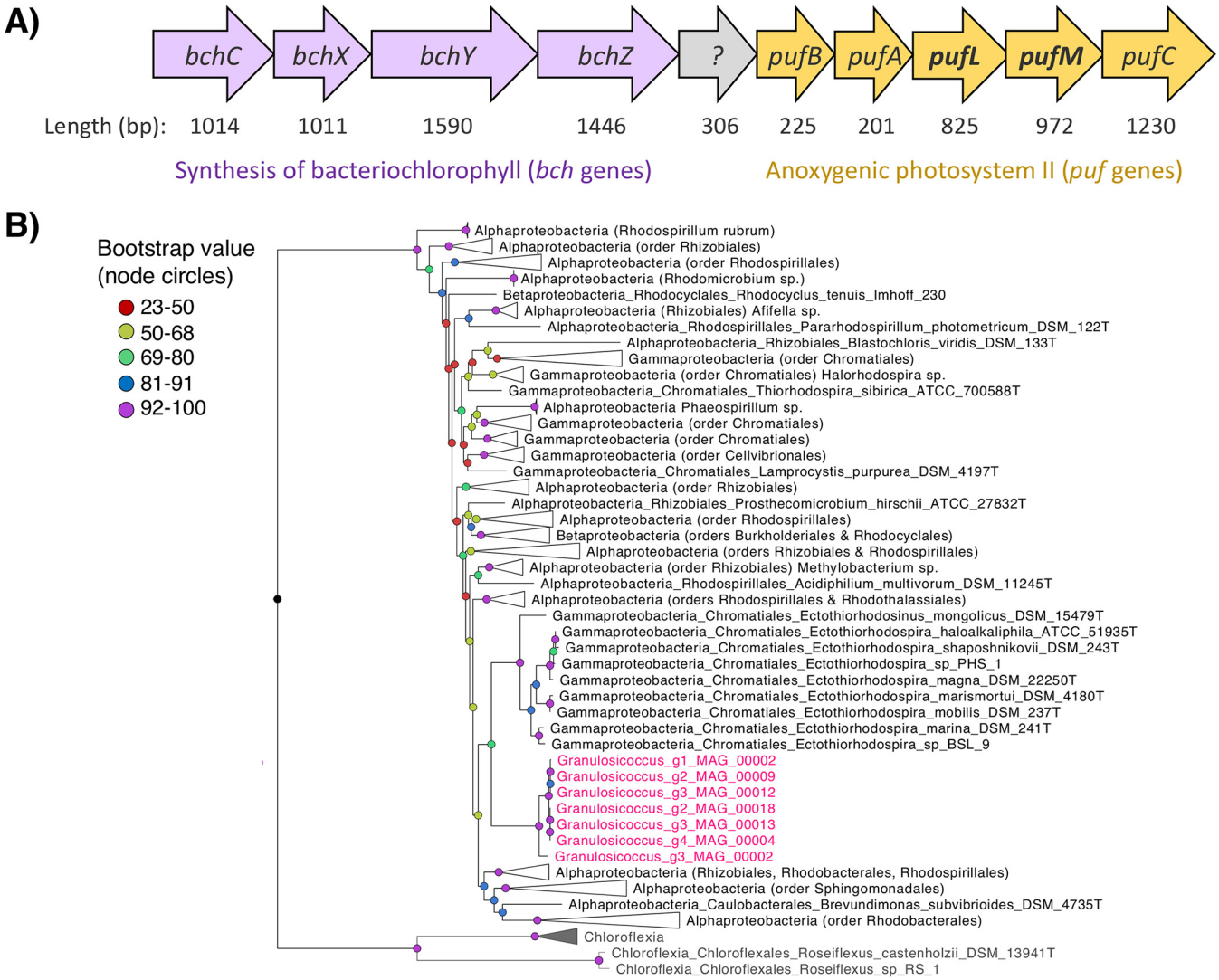

FIG 5 (A) Gene cluster containing 9 sequential genes for the synthesis of bacteriochlorophyll (*bch*) and anoxygenic photosystem II proteins (*puf*) from the genome of *Granulosicoccus* g4_MAG_00004 (contig 000000000044_split_00005). Photosystem II proteins include the light-harvesting complex 1 alpha and beta chains (*pufAB*) and the photosystem II reaction center subunits (*pufLMC*). Genes are represented by arrows, and gene lengths in nucleotide base pairs are listed below each arrow. (B) Maximum-likelihood phylogenetic tree showing the position of *Granulosicoccus pufLM* sequences (indicated in pink) in relation to photosystem II reaction center *pufLM* sequences from other known lineages of aerobic anoxygenic phototrophic bacteria. Bootstrap support values are color coded at the nodes. The clade containing sequences from *Granulosicoccus* and *Ectothiorhodospira* has a bootstrap support of 76.

Phytophthora cinnamomi (eukaryotes in the *Oomycota*, closely related to kelp), indicating that these are eukaryotic MCM genes.

***Granulosicoccus* as a new lineage of aerobic anoxygenic phototrophic bacteria.** Seven out of eight of the *Granulosicoccus* MAGs in our study contained a full suite of genes that typify the aerobic anoxygenic phototrophic bacteria (44), including genes for bacteriochlorophyll synthesis and photosystem II reaction center proteins (Fig. 5A and Table 1). There were 14 genes for bacteriochlorophyll synthesis, including magnesium chelatase (*bchHI*), bacteriochlorophyllide reductase (*bchXYZ*), and protochlorophyllide reductase (*chlLNB*) genes, and 5 genes for harvesting light energy through photosystem II reaction center proteins (*pufABC* and *pufLM*; Table 1 and Table S7). Within *Granulosicoccus* genomes, gene clusters contained 9 sequential genes encoding bacteriochlorophyll synthesis and photosystem II reaction center proteins (Fig. 5A). Surprisingly, neither *G. antarcticus* IMCC3135 nor *Granulosicoccus* MAG 002746645 had these genes, except for a single magnesium chelatase gene (*bchI*) in *G. antarcticus*, which lacks the other bacteriochlorophyll synthesis genes.

To confirm that kelp-associated *Granulosicoccus* are a novel lineage of aerobic anoxygenic phototrophic bacteria, we inferred a phylogenetic tree with the photosystem II reaction center genes (*pufL* and *pufM*) from each *Granulosicoccus* MAG together with a reference database of 167 *pufL* and *pufM* sequences from reference 44. Photosystem II protein sequences from *Granulosicoccus* MAGs in this study form a highly supported clade (bootstrap support 76) with *pufLM* sequences from *Ectothiorhodospira*, which also belong to the order *Chromatiales* (Fig. 5B). However, we note that *pufM* protein sequences within the *Proteobacteria* are closely related, and sequences from the *Alpha-*, *Beta-*, and *Gammaproteobacteria* do not form monophyletic clades (Fig. 5B).

Finally, *Granulosicoccus* does not appear to have the enzymes necessary to fix carbon with this light energy. Key enzymes for the reverse tricarboxylic acid cycle (45) were absent, including ATP citrate lyase (*aclA* and *aclB* genes) and the CO_2-fixing enzyme pyruvate ferredoxin oxidoreductase (*porABCD*). Further, *Granulosicoccus* lacks genes that encode the CO_2-fixing enzyme of the Calvin cycle, RuBisCo (*cbbLM* and *rbcLS*). Therefore, the kelp-associated *Granulosicoccus* MAGs in this study are most likely photoheterotrophs, harvesting light energy with bacteriochlorophyll and photosystem II as an extra energy source while consuming organic carbon, likely from kelp-derived DOC (Fig. 4).

DISCUSSION

Bacterial taxa persist over multiple years and distant geographic locations. *N. luetkeana* is an annual kelp species that grows from microscopic gametophytes into large sporophytes (5 to 30 m tall) by midsummer (46). Adult sporophytes generally do not survive through the winter (47), especially at very wave-exposed sites like Tatoosh Island. Despite this life history, 31 MAGs (47% of the total) were detected across multiple years on *N. luetkeana* blades from Tatoosh. This remarkable continuity demonstrates that similar bacterial genomes can persist across years on a host that is only seasonally abundant, suggesting the presence of a bacterial reservoir during the months when bull kelp sporophytes are absent. Potential reservoirs include the seawater, where kelp-associated bacteria are found at low abundances (9), rocky substrates (15), perennial kelp species (11), or overwintering kelp gametophytes, which deserve further study. Because many of the abundant MAGs and those that persisted across years contained genes for nitrogen reduction and B_{12} biosynthesis, discussed below, these abundant and persistent members of the kelp microbiome may be functionally important to the host kelp.

MAGs persisted spatially as well as temporally, with 15 MAGs (23% of the total) detected on bull kelp from Tatoosh and Squaxin populations, which are separated by the length of Puget Sound and the Strait of Juan de Fuca (~300 km). Kelp from Squaxin Island have lower bacterial cell abundances (5) and a different composition of microbes than do kelp from Tatoosh Island (9). Here, we found that *Granulosicoccus* was the most abundant MAG at both sites in 2019. However, two different genomes of *Granulosicoccus* that are likely to be distinct species were differentially abundant at each location, revealing geographic differences in species-level dynamics that are likely to be missed by 16S gene sequencing. The functional gene content was nearly identical between these two differentially abundant sequence variants of *Granulosicoccus*, indicating similar functions of the dominant bacterial taxa at these geographically separated sites.

Diverse kelp-associated bacteria have the capacity to assimilate DOM and metabolize alginate. Heterotrophic bacteria rely on organic carbon for biomass production. Canopy-forming kelp contribute significantly to the pool of dissolved organic carbon (DOC) in seawater (48) by releasing approximately 15 to 30% of their total fixed carbon as DOC (24, 25, 27, 49). We found that nearly all members of the kelp microbiome contained genes encoding DOM membrane transport proteins, which are the primary mechanism for DOM assimilation by bacteria (31). We detected the presence of 72 diverse genes for DOM assimilation across 66 unique bacterial genomes, with a median of 14 distinct genes per genome. *Granulosicoccus* genomes contained the highest number of DOM transport genes, with a range of 53 to 59 per genome. Kelp

are known to release monosaccharides including mannitol, fucose, ribose, xylose, and galactose (50, 51), and kelp-associated *Granulosicoccus* are capable of assimilating these resources (Table S4). ATP-binding cassette (ABC)-type transporters for amino acids and sugars indicate active transport into bacterial cells (33). While bacteria in the surrounding seawater also consume kelp-derived DOM (26, 27), the microbiome of the giant kelp *M. pyrifera* was enriched in transport protein genes relative to metagenomes from the surrounding seawater (21), suggesting the importance of DOM assimilation by kelp surface-associated bacteria. While we cannot infer from genomic content alone that these DOM transport proteins are being expressed, they are good indicators of potential kelp-derived DOM use by members of the kelp microbiome. Further research should use isotope tracer or culture-based studies to demonstrate that biomass production of kelp-associated bacteria is fueled by DOM released by the host kelp.

Kelp-associated bacterial genomes contained genes for alginate lyase, which degrades alginate, a brown algal cell wall polysaccharide, into oligosaccharides. Given that alginate can comprise more than 25% of kelp dry weight (52), it represents an extensive pool of organic carbon. A culture-based study from the giant kelp *Macrocystis pyrifera* reported alginate use in diverse *Gammaproteobacteria*, *Alphaproteobacteria*, and *Flavobacteriaceae* (29). Here, we found alginate lyase genes in those groups as well as the *Planctomycetes* (*Phycisphaera*) and additional families including the *Saprospiraceae*, *Granulosicoccaceae*, *Maricaulaceae*, *Sphingomonadaceae*, and UBA7415. One of the most abundant bacteria in this study, *Hellea*, was abundant on other kelps such as *Laminaria setchellii* (15) and *Laminaria hyperborea* (14). *Hellea* genomes contained many DOM assimilation and alginate lyase genes, suggesting an active role in kelp forest carbon metabolism. Surprisingly, we did not detect genes for degradation of the storage polysaccharide laminarin in kelp-associated bacterial genomes.

While some bacteria degrade alginate, others synthesize this polysaccharide as a component of biofilm or extracellular matrix formation. The pathogen *Pseudomonas aeruginosa* notoriously secretes alginate during biofilm formation in the lungs (34). Here, diverse kelp-associated bacteria contained genes encoding alginate biosynthesis proteins. One *Alphaproteobacteria* member (genus GCA-2708415) contained 5 alginate biosynthesis genes, including the *algE* gene responsible for alginate export across the outer membrane (34). Further research should investigate the role of alginate-producing bacteria in biofilm formation on diverse hosts, from the human gut to macroalgal surfaces.

Kelp-associated *Akkermansiaceae* MAGs contained many genes for sulfatases, which are key enzymes in the degradation of mucin (53) and other sulfated polysaccharides, including fucoidan (54, 55). *Akkermansiaceae* MAGs also contained genes for metabolizing the sugar *N*-acetylglucosamine, a component of mucin that is likely abundant in the kelp surface mucus layer. Members of the *Akkermansiaceae* are common symbionts in the healthy human gut, where they specialize in the degradation of mucin (56), and they likely play a similar role in the kelp microbiome. *Akkermansiaceae* are understudied in the environment but were abundant during spring diatom blooms, where they consumed sugars (55).

Kelp-associated bacteria reduce oxidized nitrogen sources to ammonium. The annual kelp *N. luetkeana* grows extraordinarily fast, producing 1 to 6 cm of new blade tissue per day (47), and rapidly assimilates dissolved inorganic nitrogen (25, 57, 58). Ammonium is the most energetically preferable form of dissolved inorganic nitrogen for algae, as it can be directly incorporated into amino acids without expending energy on intracellular nitrate reduction (59, 60). While nitrate concentrations are higher than those of ammonium on the coast of Washington during the summer (61), *N. luetkeana* blades assimilate ammonium 1.5 times faster than nitrate relative to its availability (25), indicating a preference for the more reduced form of nitrogen. Urea is a nitrogenous waste product excreted by common marine animals, including zooplankton (62), and urea can constitute a significant proportion (~20%) of the dissolved nitrogen pool in coastal seawater (63). Kelp-associated bacterial genomes from the *Proteobacteria*,

Verrucomicrobia, and *Planctomycetes* contained one or more genes for dissimilatory nitrate and nitrite reduction and urea hydrolysis (Fig. 3B), which generate ammonium as a reduced nitrogen source that may be favorable to the host kelp.

Despite the presence of these genes, it is still unknown whether ammonium generated through dissimilatory nitrate reduction or urea hydrolysis is accessible to the host kelp. Surface-associated bacteria also compete directly with the host kelp for nitrogen in the seawater (64), and kelp-associated MAGs contained assimilatory nitrate and nitrite reduction genes. While it may seem surprising to find dissimilatory nitrate reduction, an anaerobic process, associated with a photosynthetic host, kelp blades deplete oxygen at night through respiration (65), and biofilm layers can have reduced oxygen (66). Nitrate and nitrite reduction genes were also enriched in the surface microbiome of the giant kelp *M. pyrifera* compared to seawater metagenomes (21); thus, nitrate reduction may be a common function of the kelp microbiome. Future studies should test the hypothesis that kelp-associated bacteria provide reduced nitrogen to their host kelp using ^{15}N isotope tracers.

Kelp-associated *Granulosicoccus* are motile, photoheterotrophic, nitrogen- and sulfur-transforming microbes with the potential to synthesize cobalamin (B_{12}). The genus *Granulosicoccus* (order *Chromatiales*, class *Gammaproteobacteria*) currently contains 4 species isolated from Antarctic seawater (67, 68), the seagrass *Zostera marina* (69), and the kelp *Undaria pinnatifida* (70). *Granulosicoccus* is the most abundant bacterium associated with *N. luetkeana* (9), reaching densities of up to 10^6 cells per cm^2 on kelp blades (5), and it associates with diverse algal hosts (18). Only a single annotated genome is available for this bacterial genus, belonging to the free-living *Granulosicoccus antarcticus* type strain IMCC3135 (37). Here, we reconstructed 8 MAGs of *Granulosicoccus* associated with kelp blades which share, on average, only 71.9% similarity with *G. antarcticus*. The *Granulosicoccus* genomes assembled from the kelp surface likely represent 4 new species in this genus, as they formed 4 distinct clades with ANI of >98% within each clade (Fig. S2). Kelp-associated *Granulosicoccus* had large genomes of ~4.3 Mbp (Table S2), consistent with the large genome of *G. antarcticus* that is also enriched in genes for carbohydrate and amino acid transport and metabolism relative to other bacteria in the order *Chromatiales* (37).

Kelp-associated *Granulosicoccus* are motile and likely chemotactic, providing a mechanism for colonizing kelp tissues from the seawater and reaching high abundances on new kelp blade meristem tissues (5, 12, 15, 30). *Granulosicoccus* genomes contained 32 flagellar genes and 11 chemotaxis genes, including two-component system chemotaxis proteins and genes for rotation of the flagellar motor (Table S7). The motility of *G. antarcticus* is achieved through numerous tufts of flagella (67). All *Granulosicoccus* genomes also contained up to 17 type IV pilus assembly protein genes, which are known to be involved in biofilm formation and adhesion to host cells (71). On the kelp surface, *Granulosicoccus* cells are closely associated with kelp cells at the base of the biofilm (5).

Granulosicoccus belongs to the order *Chromatiales*, also known as purple sulfur bacteria because they are usually phototrophic and contain carotenoid and bacteriochlorophyll pigments (44, 72). While previous isolates of *Granulosicoccus* are obligately chemoheterotrophic (37, 67), we found genomic evidence that kelp-associated *Granulosicoccus* have the capacity to harvest light energy with bacteriochlorophyll and photosystem II reaction center proteins. Genes for CO_2 fixation were absent, suggesting a photoheterotrophic metabolism. Further, culture studies of *Granulosicoccus* show that they cannot fix carbon and require organic carbon for growth (67). PSII reaction center genes (*pufLM*) from *Granulosicoccus* MAGs formed a clade with *pufLM* genes from *Ectothiorhodospira* (Fig. 5B), another genus in the order *Chromatiales*. While many purple sulfur bacteria are anaerobic (44), *Granulosicoccus* MAGs contained genes for aerobic respiration via the citrate cycle, and *G. antarcticus* is obligately aerobic (67). Therefore, the *Granulosicoccus* from this study likely represent a novel reported lineage of aerobic anoxygenic phototrophic (AAP) bacteria. As photoheterotrophs, AAP bacteria have the capacity to generate ATP with light energy, providing extra energy for the cell that increases their growth efficiency and gives

them a competitive advantage over other heterotrophic bacteria (73–75). This energetic advantage may allow them to reach high densities and form cell clusters on kelp blade surfaces (5). Canopy kelp likely provide ideal habitats for AAP bacteria that benefit from both sunlight exposure and a constant supply of organic carbon. Other notable AAP bacteria include phytoplankton-associated *Roseobacter* bacteria (73, 76), which likely consume phytoplankton-exuded DOC (75). While AAP bacteria associated with macroalgae have a constant supply of organic carbon and may not be energy limited, we hypothesize that supplemental energy from photoheterotrophy may aid *Granulosicoccus* survival during periods of non-host association.

Granulosicoccus MAGs contained more than 50 different genes for carbohydrate and DOM transport, likely to assimilate kelp-derived dissolved organic carbon resources (25). The most complete (98.6%) *Granulosicoccus* MAG contained 22 genes for complete biosynthesis of vitamin B_{12} (cobalamin), while 7 out of 8 MAGs contained at least 10 genes for B_{12} biosynthesis. Bacteria are the only organisms known to synthesize vitamin B_{12}; thus, diverse algae rely on associated bacteria to produce vitamin B_{12} (41, 76), and brown algae are no exception (77). While a full genome of *N. luetkeana* may be necessary to confirm this finding (42), kelp host genomic content contained the B_{12}-dependent enzyme methylmalonyl-CoA mutase, which requires B_{12} as a cofactor to catalyze an essential catabolic reaction (42, 43). Interactions analogous to those described here exist between phytoplankton and heterotrophic bacteria; carbohydrates and amino acids are secreted by the phytoplankton host, and associated bacteria provide reduced nitrogen and vitamins such as B_{12} (19, 20, 78).

In summary, the genomes of kelp-associated bacteria carried carbon assimilation, polysaccharide degradation, nitrogen transformation, and vitamin biosynthesis genes that may be central to kelp-microbe interactions. Kelp forests are declining globally due to numerous environmental stressors, including ocean warming (79, 80). These climatic stressors may also impact the kelp microbiome (81), heightening our need to understand the functional role of the kelp microbiome. Kelp play a critical role as habitat-forming foundation species in temperate and arctic coastal ecosystems worldwide, and we must continue to investigate how the kelp microbiome impacts kelp fitness.

MATERIALS AND METHODS

Sample collection, DNA extraction, and metagenomic sequencing. Samples for metagenomic sequencing were obtained from individuals of the kelp *Nereocystis luetkeana* at a well-studied location on Tatoosh Island, WA, USA (48.39°N, 124.74°W), over three consecutive years. Samples were collected at the north-facing Main Beach site in July 2017, July 2018, and July 2019. In July 2019, additional *N. luetkeana* samples were collected from Squaxin Island in southern Puget Sound (47.18°N, 122.91°W), the southernmost location in Puget Sound where *N. luetkeana* persists. Previous research found a significantly different microbial community composition and reduced microbial cell density on kelp from Squaxin Island compared to those from Tatoosh Island (5, 9). In 2017 to 2018, whole tissue blade samples from Tatoosh Island were collected by removing 2 by 1 cm^2 of tissue from the middle of the kelp blade with sterile scissors. In 2019, samples from both Tatoosh and Squaxin Island *N. luetkeana* populations were collected by swabbing the middle to tip of the blade for 20 s with a sterile cotton swab. All samples were immediately frozen at −20°C and transferred to −80°C for storage.

DNA was extracted from whole kelp tissues and swabs using the DNeasy Power Soil kit (Qiagen). To acquire a sufficient quantity of DNA for metagenomic library preparation (>100 ng), DNA extracts from multiple kelp samples were pooled for each individual metagenome, with the number of pooled replicates listed in Table S1 in the supplemental material. In total, 7 metagenome samples were sequenced from *N. luetkeana* blades. DNA extracts were sent to the Argonne National Laboratory for library preparation and metagenomic sequencing on an Illumina HiSeq 2500 (2 by 150 bp).

Assembly, annotation, and binning of metagenome-assembled genomes (MAGs). The following analyses, from sequence quality control to binning, were performed within the anvi'o 7.0 environment (82, 83). All associated code is publicly available at https://github.com/brookeweigel/Kelp_associated_bacterial_genomes. First, raw sequences from forward and reverse reads were checked for sequence quality using "filter-quality-minoche" (84). For all samples, >92% of sequence reads passed quality control, and the mean number of reads per sample after quality control was 22,339,573 (Table S1). Quality sequences were assembled into contigs using IDBA-UD (85) with a minimum contig length of 1,000. Metagenomes collected from the same kelp forest location and same year were coassembled, resulting in 4 total assemblies (Table S1). We did not assemble across multiple years or locations to avoid chimeric genomes. The command "anvi-gen-contigs-database" was used to generate contigs databases, which compute k-mer frequencies and identify open reading frames with Prodigal (86). To determine the

occurrence of 22 bacterial single-copy genes in each contigs database, hidden Markov models were run using HMMER (87) with "anvi-run-hmms." Genes in each contigs database were annotated with all 3 available databases: (i) NCBI's Clusters of Orthologous Genes (COGs), (ii) EBI's Pfam database, and (iii) KEGG (Kyoto Encyclopedia of Genes and Genomes). Metagenomic short reads from all 7 samples were mapped to each of the 4 coassemblies using Bowtie2 (88), and SAMtools (89) was used to produce BAM files.

To perform metagenomic binning of contigs using anvi'o, profile databases were generated from BAM files and contigs databases using "anvi-profile" with a minimum contig length of 2,500 (to visualize all contigs), and profiles for coassembled samples were merged. To cluster contigs into MAGs, manual binning and refinement were performed using "anvi-interactive" with both sequence composition (tetranucleotide frequency) and differential coverage across all samples, following previously described approaches to generate high-quality MAGs (90, 91). For coassemblies derived from whole kelp tissue extracts, there was one large bin in each assembly consisting of genomic reads from the host kelp, which was clearly differentiated from bacterial bins based on GC content and differential coverage. Further, BLAST searching revealed that sequences from these bins had a high percent identity match to other brown alga and eukaryotic genomes. To remove host reads from further analyses, the bin containing kelp genomic reads was deselected from the final bin collection in anvi'o. While binning, microbial taxonomy was estimated within anvi'o using "anvi-run-scg-taxonomy," which searches single-copy genes from each genome against the Genome Taxonomy Database (GTDB). After binning each assembly using "anvi-interactive," bacterial bins were individually inspected using "anvi-refine," where they were checked for contaminating contig clusters with dissimilar GC content and differential coverage. Final bin collections were checked for completeness and contamination (also referred to as redundancy) using "anvi-summarize."

The final MAG collection, curated using "anvi-rename-bins," contains MAGs with >50% completion and <10% redundancy. Final MAGs were named based on the following scheme: the prefix g1 to g4 corresponds to the metagenome assembly from which it was binned (Table S1), while the numbers distinguish unique MAGs within each coassembly (e.g., g1_MAG_00001). In total, we assembled 28 high-quality MAGs (>90% completion, <5% contamination) and 51 medium-quality MAGs (>50% completion and <10% contamination), according to the genomic standards in reference 92 (Table S2).

Taxonomic assignment and curation of a nonredundant MAG data set. To identify highly similar MAGs and pick representative genomes out of the redundant MAGs, the command "anvi-dereplicate-genomes" was used to dereplicate the final MAG collection at 99% average nucleotide identity (ANI) using PyANI (93). Out of the 79 MAGs, 13 were redundant, generating a final data set of 66 nonredundant (or unique) MAGs (Table S2). Representative MAGs with the highest completion combined with the lowest redundancy were selected. Final analyses were conducted with the nonredundant MAG data set. Taxonomy was assigned to each MAG using GTDB-Tk (v1.3.0) (94), which uses a set of 120 concatenated bacterial gene markers to place MAGs in a reference tree based on the Genome Taxonomy Database (release 95) (95), using both FastANI (35) and pplacer (96). MAGs were exported from anvi'o for GTDB-Tk classification using anvi-summarize. The final maximum-likelihood phylogenetic tree was inferred using the IQ-TREE software (97) with the alignment of 120 concatenated bacterial gene markers from GTDB-Tk. Using IQ-TREE, ModelFinder (98) was first implemented to select the best-fit nucleotide substitution model (LG+F+R6), and bootstrap support values were obtained with 1,000 bootstrap replicates.

We determined the detection and abundance of nonredundant MAGs across metagenome samples using "anvi-summarize." Detection data were visualized using "anvi-interactive" with the minimum detection set to 0.70, indicating that a genome is considered present in a sample if at least 70% of nucleotides in the genome are covered by at least one short read from that sample. We visualized the abundance of nonredundant MAGs within samples using the R packages phyloseq (version 1.30) (99) and ggplot2 (version 3.3.0) (100).

Pangenomic analysis of *Granulosicoccus*. The term "pangenome" describes the genes present in all genomes of a given species, which can be subdivided into core genes that are shared by all members of a given species, and accessory genes, present in some but not all genomes of a given species (101). In this study, we generated 8 novel MAGs of *Granulosicoccus*, including 6 of high quality (>90% completion; Table S2). We generated a pangenome with these 8 MAGs, along with two publicly available *Granulosicoccus* genomes: the complete isolate genome of *Granulosicoccus antarcticus* type strain IMCC3135 (37) and *Granulosicoccus* MAG 002746645, a MAG assembled from a bottlenose dolphin's mouth (38). To compare the average nucleotide identities (ANIs) among *Granulosicoccus* genomes, we used "anvi-compute-genome-similarity" with PyANI (93). We used anvi'o to analyze and visualize the pangenome with "anvi-display-pan." First, we made a database of all 10 genomes using "anvi-gen-genomes-storage" and generated the pangenome using "anvi-pan-genome" (minbit set to 0.5 and mcl-inflation set to 10), which uses NCBI's BLAST to quantify sequence similarity within and between genomes. To obtain functional gene annotations and amino acid sequences from all genes within each *Granulosicoccus* genome, we used "anvi-summarize." Finally, to search for KEGG metabolic pathways present in the pangenome, we used "anvi-estimate-metabolism" with an E value threshold of 1e−05 and a bitscore fraction of 0.5.

Functional gene presence-absence across all MAGs. We constructed a database of annotated genes (COG, KEGG, and Pfam) in each MAG based on anvi'o-generated tables and quantified the number of genes annotated with a given function in each MAG using custom python scripts (for example, see https://github.com/kkmiranda/PNWMetagenomes/blob/main/microbial_metabolisms/finalNitro.py). We searched for genes involved in dissolved organic matter (DOM) transport (list adapted from reference 31), nitrogen metabolism and transformation (56 genes, including those involved in nitrogen fixation, assimilatory and dissimilatory nitrate reduction, denitrification, nitrification, comammox, and urea

hydrolysis), and vitamin B_{12} synthesis (list adapted from references 76 and 102) and genes encoding laminarin and alginate metabolism enzymes. E values are the expected number of false-positive hits for a gene annotation, adjusted to the sequence database size. We used E value cutoffs of 1e−20 for KEGG annotations and 1e−50 for COG annotations. We visualized the presence-absence of functional genes across MAGs with heatmaps generated using "anvi-interactive," where the python-generated functional gene tables were imported as additional layers.

Phylogenetic analysis of photosystem II (*pufLM*) genes. To validate the presence of genes for aerobic anoxygenic phototrophy (AAP) in *Granulosicoccus* MAGs and determine their relationship to other known AAP bacteria, we extracted amino acid sequences for the *pufL* and *pufM* photosystem II reaction center genes from each MAG using "anvi-summarize." We acquired a reference database of 167 *pufL* and *pufM* sequences from reference 44 including 99 belonging to the *Alphaproteobacteria*, 14 to the *Betaproteobacteria*, and 49 to the *Gammaproteobacteria* and 5 from the phylum *Chloroflexi* that were used as an outgroup, as in reference 72. Concatenated *pufLM* sequences were aligned using MAFFT v7.309 (103). A maximum-likelihood phylogeny was inferred using IQ-TREE (97), with ModelFinder (98) to select the best-fit nucleotide substitution model, partitioned for *pufL* and *pufM* genes. Model selection resulted in the best-fit model of LG+F+I+G4 across both genes, and bootstrap support values were obtained with 1,000 bootstrap replicates.

Data availability. In addition to the code available on GitHub, the final MAG database files generated in anvi'o are available on the Figshare repository: https://figshare.com/s/84c036dc253a5dd1b1b9. Metagenomic sequence data and bacterial genomes are available at the NCBI's Sequence Read Archive under accession no. PRJNA783443, including the 7 metagenomes (BioSample accession numbers SAMN23429948 to SAMN23429954) and the 66 nonredundant metagenome-assembled genomes (SAMN27917399 to SAMN27917464).

SUPPLEMENTAL MATERIAL

Supplemental material is available online only.

FIG S1, TIF file, 1.4 MB.
FIG S2, TIF file, 0.4 MB.
FIG S3, TIF file, 1.1 MB.
TABLE S1, XLSX file, 0.01 MB.
TABLE S2, XLSX file, 0.02 MB.
TABLE S3, XLSX file, 0.02 MB.
TABLE S4, XLSX file, 0.03 MB.
TABLE S5, XLSX file, 0.04 MB.
TABLE S6, XLSX file, 0.01 MB.
TABLE S7, XLSX file, 0.02 MB.

ACKNOWLEDGMENTS

We are grateful to the Makah Tribal Nation for access to Tatoosh Island and to the Squaxin Island Tribe for access to kelp from Squaxin Island. Thanks to Helen Berry for facilitating boat access to South Puget Sound, and thanks to Olivia Cattau for help with kelp collections. Thanks to Stephanie Greenwald and Sarah Owens at Argonne National Lab for providing expertise in metagenomic sequencing. Conversations with the Meren lab and responses on the anv'io Slack channel greatly assisted our data analysis. Thanks to Maureen Coleman and Justin Podowski for helpful conversations about microbial ecology and nitrogen cycling.

This research was supported by the Climate Change Initiative funded by the Rebecca Susan Buffett Foundation, a Phycological Society of America Grant awarded to B.L.W., NOAA-COCA (no. NA160AR431055), a Washington Department of Natural Resources (no. 93099282) grant awarded to C.A.P., and an NSF-DEB grant (no. 1556874) awarded to J. T. Wootton. B.L.W. was supported by a GAANN fellowship from the Department of Education, by the Washington State DNR, and by a travel award from the Committee on Evolutionary Biology at the University of Chicago.

REFERENCES

1. Wheeler WN, Druehl LD. 1986. Seasonal growth and productivity of Macrocystis integrifolia in British Columbia, Canada. Mar Biol 90:181–186. https://doi.org/10.1007/BF00569125.
2. Graham MH, Vasquez JA, Buschmann AH. 2007. Global ecology of the giant kelp Macrocystis: from ecotypes to ecosystems. Oceanogr Mar Biol Annu Rev 45:39–88.
3. Steneck RS, Graham MH, Bourque BJ, Corbett D, Erlandson JM, Estes JA, Tegner MJ. 2002. Kelp forest ecosystems: biodiversity, stability, resilience and future. Environ Conserv 29:436–459. https://doi.org/10.1017/S0376892902000322.
4. Bengtsson MM, Øvreås L. 2010. Planctomycetes dominate biofilms on surfaces of the kelp Laminaria hyperborea. BMC Microbiol 10:261. https://doi.org/10.1186/1471-2180-10-261.
5. Ramírez-Puebla ST, Weigel BL, Jack L, Schlundt C, Pfister CA, Mark Welch JL. 2022. Spatial organization of the kelp microbiome at micron scales. Microbiome 10:52. https://doi.org/10.1186/s40168-022-01235-w.

6. Beinart RA. 2019. The significance of microbial symbionts in ecosystem processes. mSystems 4:e00127-19. https://doi.org/10.1128/mSystems.00127-19.
7. Egan S, Harder T, Burke C, Steinberg P, Kjelleberg S, Thomas T. 2013. The seaweed holobiont: understanding seaweed–bacteria interactions. FEMS Microbiol Rev 37:462–476. https://doi.org/10.1111/1574-6976.12011.
8. Michelou VK, Caporaso JG, Knight R, Palumbi SR. 2013. The ecology of microbial communities associated with Macrocystis pyrifera. PLoS One 8:e67480. https://doi.org/10.1371/journal.pone.0067480.
9. Weigel BL, Pfister CA. 2019. Successional dynamics and seascape-level patterns of microbial communities on the canopy-forming kelps Nereocystis luetkeana and Macrocystis pyrifera. Front Microbiol 10:346. https://doi.org/10.3389/fmicb.2019.00346.
10. Florez JZ, Camus C, Hengst MB, Buschmann AH. 2017. A functional perspective analysis of macroalgae and epiphytic bacterial community interaction. Front Microbiol 8:2561. https://doi.org/10.3389/fmicb.2017.02561.
11. Lemay MA, Martone PT, Keeling PJ, Burt JM, Krumhansl KA, Sanders RD, Wegener Parfrey L. 2018. Sympatric kelp species share a large portion of their surface bacterial communities. Environ Microbiol 20:658–670. https://doi.org/10.1111/1462-2920.13993.
12. Bengtsson MM, Sjøtun K, Lanzén A, Øvreås L. 2012. Bacterial diversity in relation to secondary production and succession on surfaces of the kelp Laminaria hyperborea. ISME J 6:2188–2198. https://doi.org/10.1038/ismej.2012.67.
13. James AK, English CJ, Nidzieko NJ, Carlson CA, Wilbanks EG. 2020. Giant kelp microbiome altered in the presence of epiphytes. Limnol Oceanogr Lett 5:354–362. https://doi.org/10.1002/lol2.10157.
14. Brunet M, Bettignies F, Le Duff N, Tanguy G, Davoult D, Leblanc C, Gobet A, Thomas F. 2021. Accumulation of detached kelp biomass in a subtidal temperate coastal ecosystem induces succession of epiphytic and sediment bacterial communities. Environ Microbiol 23:1638–1655. https://doi.org/10.1111/1462-2920.15389.
15. Lemay MA, Davis KM, Martone PT, Parfrey LW. 2021. Kelp-associated microbiota are structured by host anatomy. J Phycol 57:1119–1130. https://doi.org/10.1111/jpy.13169.
16. Quigley CTC, Capistrant-Fossa KA, Morrison HG, Johnson LE, Morozov A, Hertzberg VS, Brawley SH. 2020. Bacterial communities show algal host (Fucus spp.)/zone differentiation across the stress gradient of the intertidal zone. Front Microbiol 11:563118. https://doi.org/10.3389/fmicb.2020.563118.
17. Capistrant-Fossa KA, Morrison HG, Engelen AH, Quigley CTC, Morozov A, Serrão EA, Brodie J, Gachon CMM, Badis Y, Johnson LE, Hoarau G, Abreu MH, Tester PA, Stearns LA, Brawley SH. 2021. The microbiome of the habitat-forming brown alga Fucus vesiculosus (Phaeophyceae) has similar cross-Atlantic structure that reflects past and present drivers. J Phycol 57:1681–1698. https://doi.org/10.1111/jpy.13194.
18. Singh RP, Reddy CRK. 2014. Seaweed-microbial interactions: key functions of seaweed-associated bacteria. FEMS Microbiol Ecol 88:213–230. https://doi.org/10.1111/1574-6941.12297.
19. Amin SA, Hmelo LR, van Tol HM, Durham BP, Carlson LT, Heal KR, Morales RL, Berthiaume CT, Parker MS, Djunaedi B, Ingalls AE, Parsek MR, Moran MA, Armbrust EV. 2015. Interaction and signalling between a cosmopolitan phytoplankton and associated bacteria. Nature 522:98–101. https://doi.org/10.1038/nature14488.
20. Seymour JR, Amin SA, Raina J-B, Stocker R. 2017. Zooming in on the phycosphere: the ecological interface for phytoplankton–bacteria relationships. Nat Microbiol 2:17065. https://doi.org/10.1038/nmicrobiol.2017.65.
21. Minich JJ, Morris MM, Brown M, Doane M, Edwards MS, Michael TP, Dinsdale EA. 2018. Elevated temperature drives kelp microbiome dysbiosis, while elevated carbon dioxide induces water microbiome disruption. PLoS One 13:e0192772. https://doi.org/10.1371/journal.pone.0192772.
22. Hamersley MR, Sohm JA, Burns JA, Capone DG. 2015. Nitrogen fixation associated with the decomposition of the giant kelp Macrocystis pyrifera. Aquat Bot 125:57–63. https://doi.org/10.1016/j.aquabot.2015.05.003.
23. Florez JZ, Camus C, Hengst MB, Buschmann AH. 2021. A mesocosm study on bacteria-kelp interactions: importance of nitrogen availability and kelp genetics. J Phycol 57:1777–1791. https://doi.org/10.1111/jpy.13213.
24. Reed DC, Carlson CA, Halewood ER, Nelson JC, Harrer SL, Rassweiler A, Miller RJ. 2015. Patterns and controls of reef-scale production of dissolved organic carbon by giant kelp Macrocystis pyrifera. Limnol Oceanogr 60:1996–2008. https://doi.org/10.1002/lno.10154.
25. Weigel BL, Pfister CA. 2021. The dynamics and stoichiometry of dissolved organic carbon release by kelp. Ecology 102:e03221. https://doi.org/10.1002/ecy.3221.
26. Thomas F, Le Duff N, Wu T-D, Cébron A, Uroz S, Riera P, Leroux C, Tanguy G, Legeay E, Guerquin-Kern J-L. 2021. Isotopic tracing reveals single-cell assimilation of a macroalgal polysaccharide by a few marine Flavobacteria and Gammaproteobacteria. ISME J 15:3062–3075. https://doi.org/10.1038/s41396-021-00987-x.
27. Gao Y, Zhang Y, Du M, Lin F, Jiang W, Li W, Li F, Lv X, Fang J, Jiang Z. 2021. Dissolved organic carbon from cultured kelp Saccharina japonica: production, bioavailability, and bacterial degradation rates. Aquacult Environ Interact 13:101–110. https://doi.org/10.3354/aei00393.
28. Bengtsson M, Sjøtun K, Storesund J, Øvreås J. 2011. Utilization of kelp-derived carbon sources by kelp surface-associated bacteria. Aquat Microb Ecol 62:191–199. https://doi.org/10.3354/ame01477.
29. Lin JD, Lemay MA, Parfrey LW. 2018. Diverse bacteria utilize alginate within the microbiome of the giant kelp Macrocystis pyrifera. Front Microbiol 9:1914. https://doi.org/10.3389/fmicb.2018.01914.
30. Weigel BL, Pfister CA. 2021. Oxygen metabolism shapes microbial settlement on photosynthetic kelp blades compared to artificial kelp substrates. Environ Microbiol Rep 13:176–184. https://doi.org/10.1111/1758-2229.12923.
31. Poretsky RS, Sun S, Mou X, Moran MA. 2010. Transporter genes expressed by coastal bacterioplankton in response to dissolved organic carbon. Environ Microbiol 12:616–627. https://doi.org/10.1111/j.1462-2920.2009.02102.x.
32. Bergauer K, Fernandez-Guerra A, Garcia JAL, Sprenger RR, Stepanauskas R, Pachiadaki MG, Jensen ON, Herndl GJ. 2018. Organic matter processing by microbial communities throughout the Atlantic water column as revealed by metaproteomics. Proc Natl Acad Sci U S A 115:E400–E408. https://doi.org/10.1073/pnas.1708779115.
33. Rees DC, Johnson E, Lewinson O. 2009. ABC transporters: the power to change. Nat Rev Mol Cell Biol 10:218–227. https://doi.org/10.1038/nrm2646.
34. Whitney JC, Hay ID, Li C, Eckford PDW, Robinson H, Amaya MF, Wood LF, Ohman DE, Bear CE, Rehm BH, Howell PL. 2011. Structural basis for alginate secretion across the bacterial outer membrane. Proc Natl Acad Sci U S A 108:13083–13088. https://doi.org/10.1073/pnas.1104984108.
35. Jain C, Rodriguez-R LM, Phillippy AM, Konstantinidis KT, Aluru S. 2018. High throughput ANI analysis of 90K prokaryotic genomes reveals clear species boundaries. Nat Commun 9:5114. https://doi.org/10.1038/s41467-018-07641-9.
36. Barco RA, Garrity GM, Scott JJ, Amend JP, Nealson KH, Emerson D. 2020. A genus definition for Bacteria and Archaea based on a standard genome relatedness index. mBio 11:e02475-19. https://doi.org/10.1128/mBio.02475-19.
37. Kang I, Lim Y, Cho J-C. 2018. Complete genome sequence of Granulosicoccus antarcticus type strain IMCC3135T, a marine gammaproteobacterium with a putative dimethylsulfoniopropionate demethylase gene. Mar Genomics 37:176–181. https://doi.org/10.1016/j.margen.2017.11.005.
38. Dudek NK, Sun CL, Burstein D, Kantor RS, Aliaga Goltsman DS, Bik EM, Thomas BC, Banfield JF, Relman DA. 2017. Novel microbial diversity and functional potential in the marine mammal oral microbiome. Curr Biol 27:3752–3762.e6. https://doi.org/10.1016/j.cub.2017.10.040.
39. Kojima H, Fukui M. 2016. Sulfuriflexus mobilis gen. nov., sp. nov., a sulfur-oxidizing bacterium isolated from a brackish lake sediment. Int J Syst Evol Microbiol 66:3515–3518. https://doi.org/10.1099/ijsem.0.001227.
40. Yoch DC. 2002. Dimethylsulfoniopropionate: its sources, role in the marine food web, and biological degradation to dimethylsulfide. Appl Environ Microbiol 68:5804–5815. https://doi.org/10.1128/AEM.68.12.5804-5815.2002.
41. Croft MT, Lawrence AD, Raux-Deery E, Warren MJ, Smith AG. 2005. Algae acquire vitamin B12 through a symbiotic relationship with bacteria. Nature 438:90–93. https://doi.org/10.1038/nature04056.
42. Helliwell KE, Wheeler GL, Leptos KC, Goldstein RE, Smith AG. 2011. Insights into the evolution of vitamin B12 auxotrophy from sequenced algal genomes. Mol Biol Evol 28:2921–2933. https://doi.org/10.1093/molbev/msr124.
43. Grossman A. 2016. Nutrient acquisition: the generation of bioactive vitamin B 12 by microalgae. Curr Biol 26:R319–R321. https://doi.org/10.1016/j.cub.2016.02.047.
44. Imhoff JF, Rahn T, Künzel S, Neulinger SC. 2018. Photosynthesis is widely distributed among Proteobacteria as demonstrated by the phylogeny of

pufLM reaction center proteins. Front Microbiol 8:2679. https://doi.org/10.3389/fmicb.2017.02679.
45. Campbell BJ, Cary SC. 2004. Abundance of reverse tricarboxylic acid cycle genes in free-living microorganisms at deep-sea hydrothermal vents. Appl Environ Microbiol 70:6282–6289. https://doi.org/10.1128/AEM.70.10.6282-6289.2004.
46. Foreman RE. 1984. Studies on Nereocystis growth in British Columbia, Canada. Hydrobiologia 116-117:325–332. https://doi.org/10.1007/BF00027696.
47. Maxell BA, Miller KA. 1996. Demographic studies of the annual kelps Nereocystis luetkeana and Costaria costata (Laminariales, Phaeophyta) in Puget Sound, Washington. Bot Mar 39:479–490. https://doi.org/10.1515/botm.1996.39.1-6.479.
48. Pfister CA, Altabet MA, Weigel BL. 2019. Kelp beds and their local effects on seawater chemistry, productivity, and microbial communities. Ecology 100:e02798. https://doi.org/10.1002/ecy.2798.
49. Miranda KK, Weigel BL, McCoy SJ, Pfister CA. 2021. Differential impacts of alternate primary producers on carbon cycling. Ecology 102:e03455. https://doi.org/10.1002/ecy.3455.
50. Newell RC, Lucas MI, Velimirov B, Seiderer LJ. 1980. Quantitative significance of dissolved organic losses following fragmentation of kelp (Ecklonia maxima and Laminaria pallida). Mar Ecol Prog Ser 2:45–59. https://doi.org/10.3354/meps002045.
51. Wada S, Aoki MN, Tsuchiya Y, Sato T, Shinagawa H, Hama T. 2007. Quantitative and qualitative analyses of dissolved organic matter released from Ecklonia cava Kjellman, in Oura Bay, Shimoda, Izu Peninsula, Japan. J Exp Mar Biol Ecol 349:344–358. https://doi.org/10.1016/j.jembe.2007.05.024.
52. Hellebust JA, Haug A. 1972. Photosynthesis, translocation, and alginic acid synthesis in Laminaria digitata and Laminaria hyperborea. Can J Bot 50:169–176. https://doi.org/10.1139/b72-022.
53. Luis AS, Jin C, Pereira GV, Glowacki RWP, Gugel SR, Singh S, Byrne DP, Pudlo NA, London JA, Baslé A, Reihill M, Oscarson S, Eyers PA, Czjzek M, Michel G, Barbeyron T, Yates EA, Hansson GC, Karlsson NG, Cartmell A, Martens EC. 2021. A single sulfatase is required to access colonic mucin by a gut bacterium. Nature 598:332–337. https://doi.org/10.1038/s41586-021-03967-5.
54. Sichert A, Corzett CH, Schechter MS, Unfried F, Markert S, Becher D, Fernandez-Guerra A, Liebeke M, Schweder T, Polz MF, Hehemann J-H. 2020. Verrucomicrobia use hundreds of enzymes to digest the algal polysaccharide fucoidan. Nat Microbiol 5:1026–1039. https://doi.org/10.1038/s41564-020-0720-2.
55. Orellana LH, Francis TB, Ferraro M, Hehemann J-H, Fuchs BM, Amann RI. 2022. Verrucomicrobiota are specialist consumers of sulfated methyl pentoses during diatom blooms. ISME J 16:630–641. https://doi.org/10.1038/s41396-021-01105-7.
56. Karcher N, Nigro E, Punčochář M, Blanco-Míguez A, Ciciani M, Manghi P, Zolfo M, Cumbo F, Manara S, Golzato D, Cereseto A, Arumugam M, Bui TPN, Tytgat HLP, Valles-Colomer M, de Vos WM, Segata N. 2021. Genomic diversity and ecology of human-associated Akkermansia species in the gut microbiome revealed by extensive metagenomic assembly. Genome Biol 22:209. https://doi.org/10.1186/s13059-021-02427-7.
57. Gerard VA. 1982. In situ water motion and nutrient uptake by the giant kelp Macrocystis pyrifera. Mar Biol 69:51–54. https://doi.org/10.1007/BF00396960.
58. Ahn O, Petrell RJ, Harrison PJ. 1998. Ammonium and nitrate uptake by Laminaria saccharina and Nereocystis luetkeana originating from a salmon sea cage farm. J Appl Phycol 10:333–340. https://doi.org/10.1023/A:1008092521651.
59. Solomonson LP, Barber MJ. 1990. Assimilatory nitrate reductase: functional properties and regulation. Annu Rev Plant Physiol Plant Mol Biol 41:225–253. https://doi.org/10.1146/annurev.pp.41.060190.001301.
60. Lobban CS, Harrison PJ. 1994. Seaweed ecology and physiology, p 163–209. Cambridge University Press, Cambridge, United Kingdom.
61. Pfister CA, Wootton JT, Neufeld CJ. 2007. Relative roles of coastal and oceanic processes in determining physical and chemical characteristics of an intensively sampled nearshore system. Limnol Oceanogr 52:1767–1775. https://doi.org/10.4319/lo.2007.52.5.1767.
62. Cass CJ, Daly KL. 2014. Eucalanoid copepod metabolic rates in the oxygen minimum zone of the eastern tropical north Pacific: effects of oxygen and temperature. Deep Sea Res I Oceanogr Res Pap 94:137–149. https://doi.org/10.1016/j.dsr.2014.09.003.
63. Smith JM, Brzezinski MA, Melack JM, Miller RJ, Reed DC. 2018. Urea as a source of nitrogen to giant kelp (Macrocystis pyrifera). Limnol Oceanogr Lett 3:365–373. https://doi.org/10.1002/lol2.10088.
64. Kirchman DL. 1994. The uptake of inorganic nutrients by heterotrophic bacteria. Microb Ecol 28:255–271. https://doi.org/10.1007/BF00166816.
65. Noisette F, Hurd C. 2018. Abiotic and biotic interactions in the diffusive boundary layer of kelp blades create a potential refuge from ocean acidification. Funct Ecol 32:1329–1342. https://doi.org/10.1111/1365-2435.13067.
66. Noisette F, Depetris A, Kühl M, Brodersen KE. 2020. Flow and epiphyte growth effects on the thermal, optical and chemical microenvironment in the leaf phyllosphere of seagrass (*Zostera marina*). J R Soc Interface 17:20200485. https://doi.org/10.1098/rsif.2020.0485.
67. Lee HK, Choi T-H, Kim K-M, Cho J-C. 2007. Granulosicoccaceae fam. nov., to include Granulosicoccus antarcticus gen. nov., sp. nov., a non-phototrophic, obligately aerobic chemoheterotroph in the order Chromatiales, isolated from Antarctic seawater. J Microbiol Biotechnol 17:1483–1490.
68. Baek K, Choi A, Kang I, Im M, Cho J-C. 2014. Granulosicoccus marinus sp. nov., isolated from Antarctic seawater, and emended description of the genus Granulosicoccus. Int J Syst Evol Microbiol 64:4103–4108. https://doi.org/10.1099/ijs.0.070045-0.
69. Kurilenko VV, Christen R, Zhukova NV, Kalinovskaya NI, Mikhailov VV, Crawford RJ, Ivanova EP. 2010. Granulosicoccus coccoides sp. nov., isolated from leaves of seagrass (Zostera marina). Int J Syst Evol Microbiol 60:972–976. https://doi.org/10.1099/ijs.0.013516-0.
70. Park S, Jung Y-T, Won S-M, Park J-M, Yoon J-H. 2014. Granulosicoccus undariae sp. nov., a member of the family Granulosicoccaceae isolated from a brown algae reservoir and emended description of the genus Granulosicoccus. Antonie Van Leeuwenhoek 106:845–852. https://doi.org/10.1007/s10482-014-0254-9.
71. Ligthart K, Belzer C, de Vos WM, Tytgat HLP. 2020. Bridging bacteria and the gut: functional aspects of type IV pili. Trends Microbiol 28:340–348. https://doi.org/10.1016/j.tim.2020.02.003.
72. Tank M, Thiel V, Imhoff JF. 2009. Phylogenetic relationship of phototrophic purple sulfur bacteria according to pufL and pufM genes. Int Microbiol 12:175–185.
73. Koblížek M. 2015. Ecology of aerobic anoxygenic phototrophs in aquatic environments. FEMS Microbiol Rev 39:854–870. https://doi.org/10.1093/femsre/fuv032.
74. Ferrera I, Sánchez O, Kolářová E, Koblížek M, Gasol JM. 2017. Light enhances the growth rates of natural populations of aerobic anoxygenic phototrophic bacteria. ISME J 11:2391–2393. https://doi.org/10.1038/ismej.2017.79.
75. Piwosz K, Vrdoljak A, Frenken T, González-Olalla JM, Šantić D, McKay RM, Spilling K, Guttman L, Znachor P, Mujakić I, Fecskeová LK, Zoccarato L, Hanusová M, Pessina A, Reich T, Grossart H-P, Koblížek M. 2020. Light and primary production shape bacterial activity and community composition of aerobic anoxygenic phototrophic bacteria in a microcosm experiment. mSphere 5:e00354-20. https://doi.org/10.1128/mSphere.00354-20.
76. Wagner-Döbler I, Ballhausen B, Berger M, Brinkhoff T, Buchholz I, Bunk B, Cypionka H, Daniel R, Drepper T, Gerdts G, Hahnke S, Han C, Jahn D, Kalhoefer D, Kiss H, Klenk H-P, Kyrpides N, Liebl W, Liesegang H, Meincke L, Pati A, Petersen J, Piekarski T, Pommerenke C, Pradella S, Pukall R, Rabus R, Stackebrandt E, Thole S, Thompson L, Tielen P, Tomasch J, von Jan M, Wanphrut N, Wichels A, Zech H, Simon M. 2010. The complete genome sequence of the algal symbiont Dinoroseobacter shibae: a hitchhiker's guide to life in the sea. ISME J 4:61–77. https://doi.org/10.1038/ismej.2009.94.
77. Dogs M, Wemheuer B, Wolter L, Bergen N, Daniel R, Simon M, Brinkhoff T. 2017. Rhodobacteraceae on the marine brown alga Fucus spiralis are abundant and show physiological adaptation to an epiphytic lifestyle. Syst Appl Microbiol 40:370–382. https://doi.org/10.1016/j.syapm.2017.05.006.
78. Luo H, Moran MA. 2014. Evolutionary ecology of the marine Roseobacter clade. Microbiol Mol Biol Rev 78:573–587. https://doi.org/10.1128/MMBR.00020-14.
79. Filbee-Dexter K, Wernberg T. 2018. Rise of turfs: a new battlefront for globally declining kelp forests. Bioscience 68:64–76. https://doi.org/10.1093/biosci/bix147.
80. Smale DA. 2020. Impacts of ocean warming on kelp forest ecosystems. New Phytol 225:1447–1454. https://doi.org/10.1111/nph.16107.
81. Qiu Z, Coleman MA, Provost E, Campbell AH, Kelaher BP, Dalton SJ, Thomas T, Steinberg PD, Marzinelli EM. 2019. Future climate change is predicted to affect the microbiome and condition of habitat-forming kelp. Proc Biol Sci 286:20181887. https://doi.org/10.1098/rspb.2018.1887.
82. Eren AM, Esen ÖC, Quince C, Vineis JH, Morrison HG, Sogin ML, Delmont TO. 2015. Anvi'o: an advanced analysis and visualization platform for 'omics data. PeerJ 3:e1319. https://doi.org/10.7717/peerj.1319.

83. Eren AM, Kiefl E, Shaiber A, Veseli I, Miller SE, Schechter MS, Fink I, Pan JN, Yousef M, Fogarty EC, Trigodet F, Watson AR, Esen ÖC, Moore RM, Clayssen Q, Lee MD, Kivenson V, Graham ED, Merrill BD, Karkman A, Blankenberg D, Eppley JM, Sjödin A, Scott JJ, Vázquez-Campos X, McKay LJ, McDaniel EA, Stevens SLR, Anderson RE, Fuessel J, Fernandez-Guerra A, Maignien L, Delmont TO, Willis AD. 2021. Community-led, integrated, reproducible multi-omics with anvi'o. Nat Microbiol 6:3–6. https://doi.org/10.1038/s41564-020-00834-3.
84. Minoche AE, Dohm JC, Himmelbauer H. 2011. Evaluation of genomic high-throughput sequencing data generated on Illumina HiSeq and Genome Analyzer systems. Genome Biol 12:R112. https://doi.org/10.1186/gb-2011-12-11-r112.
85. Peng Y, Leung HCM, Yiu SM, Chin FYL. 2012. IDBA-UD: a de novo assembler for single-cell and metagenomic sequencing data with highly uneven depth. Bioinformatics 28:1420–1428. https://doi.org/10.1093/bioinformatics/bts174.
86. Hyatt D, Chen G-L, LoCascio PF, Land ML, Larimer FW, Hauser LJ. 2010. Prodigal: prokaryotic gene recognition and translation initiation site identification. BMC Bioinformatics 11:119. https://doi.org/10.1186/1471-2105-11-119.
87. Eddy SR. 2011. Accelerated profile HMM searches. PLoS Comput Biol 7:e1002195. https://doi.org/10.1371/journal.pcbi.1002195.
88. Langmead B, Salzberg SL. 2012. Fast gapped-read alignment with Bowtie 2. Nat Methods 9:357–359. https://doi.org/10.1038/nmeth.1923.
89. Li H, Handsaker B, Wysoker A, Fennell T, Ruan J, Homer N, Marth G, Abecasis G, Durbin R, 1000 Genome Project Data Processing Subgroup. 2009. The sequence alignment/map format and SAMtools. Bioinformatics 25:2078–2079. https://doi.org/10.1093/bioinformatics/btp352.
90. Delmont TO, Quince C, Shaiber A, Esen ÖC, Lee ST, Rappé MS, McLellan SL, Lücker S, Eren AM. 2018. Nitrogen-fixing populations of Planctomycetes and Proteobacteria are abundant in surface ocean metagenomes. Nat Microbiol 3:804–813. https://doi.org/10.1038/s41564-018-0176-9.
91. Shaiber A, Willis AD, Delmont TO, Roux S, Chen L-X, Schmid AC, Yousef M, Watson AR, Lolans K, Esen ÖC, Lee STM, Downey N, Morrison HG, Dewhirst FE, Mark Welch JL, Eren AM. 2020. Functional and genetic markers of niche partitioning among enigmatic members of the human oral microbiome. Genome Biol 21:292. https://doi.org/10.1186/s13059-020-02195-w.
92. Bowers RM, Kyrpides NC, Stepanauskas R, Harmon-Smith M, Doud D, Reddy TBK, Schulz F, Jarett J, Rivers AR, Eloe-Fadrosh EA, Tringe SG, Ivanova NN, Copeland A, Clum A, Becraft ED, Malmstrom RR, Birren B, Podar M, Bork P, Weinstock GM, Garrity GM, Dodsworth JA, Yooseph S, Sutton G, Glöckner FO, Gilbert JA, Nelson WC, Hallam SJ, Jungbluth SP, Ettema TJG, Tighe S, Konstantinidis KT, Liu W-T, Baker BJ, Rattei T, Eisen JA, Hedlund B, McMahon KD, Fierer N, Knight R, Finn R, Cochrane G, Karsch-Mizrachi I, Tyson GW, Rinke C, Genome Standards Consortium, Lapidus A, Meyer F, Yilmaz P, Parks DH, Murat Eren A, Schriml L, Banfield JF, Hugenholtz P, Woyke T. 2017. Minimum information about a single amplified genome (MISAG) and a metagenome-assembled genome (MIMAG) of bacteria and archaea. Nat Biotechnol 35:725–731. https://doi.org/10.1038/nbt.3893.
93. Pritchard L, Glover RH, Humphris S, Elphinstone JG, Toth IK. 2016. Genomics and taxonomy in diagnostics for food security: soft-rotting enterobacterial plant pathogens. Anal Methods 8:12–24. https://doi.org/10.1039/C5AY02550H.
94. Chaumeil P-A, Mussig AJ, Hugenholtz P, Parks DH. 2019. GTDB-Tk: a toolkit to classify genomes with the Genome Taxonomy Database. Bioinformatics 36:1925–1927. https://doi.org/10.1093/bioinformatics/btz848.
95. Parks DH, Chuvochina M, Chaumeil P-A, Rinke C, Mussig AJ, Hugenholtz P. 2020. A complete domain-to-species taxonomy for Bacteria and Archaea. Nat Biotechnol 38:1079–1086. https://doi.org/10.1038/s41587-020-0501-8.
96. Matsen FA, Kodner RB, Armbrust EV. 2010. pplacer: linear time maximum-likelihood and Bayesian phylogenetic placement of sequences onto a fixed reference tree. BMC Bioinformatics 11:538. https://doi.org/10.1186/1471-2105-11-538.
97. Nguyen L-T, Schmidt HA, von Haeseler A, Minh BQ. 2015. IQ-TREE: a fast and effective stochastic algorithm for estimating maximum-likelihood phylogenies. Mol Biol Evol 32:268–274. https://doi.org/10.1093/molbev/msu300.
98. Kalyaanamoorthy S, Minh BQ, Wong TKF, von Haeseler A, Jermiin LS. 2017. ModelFinder: fast model selection for accurate phylogenetic estimates. Nat Methods 14:587–589. https://doi.org/10.1038/nmeth.4285.
99. McMurdie PJ, Holmes S. 2013. phyloseq: an R package for reproducible interactive analysis and graphics of microbiome census data. PLoS One 8:e61217. https://doi.org/10.1371/journal.pone.0061217.
100. Wickham H. 2016. ggplot2: elegant graphics for data analysis. Springer-Verlag, New York, NY.
101. Brockhurst MA, Harrison E, Hall JPJ, Richards T, McNally A, MacLean C. 2019. The ecology and evolution of pangenomes. Curr Biol 29:R1094–R1103. https://doi.org/10.1016/j.cub.2019.08.012.
102. Lu X, Heal KR, Ingalls AE, Doxey AC, Neufeld JD. 2020. Metagenomic and chemical characterization of soil cobalamin production. ISME J 14:53–66. https://doi.org/10.1038/s41396-019-0502-0.
103. Katoh K, Standley DM. 2013. MAFFT multiple sequence alignment software version 7: improvements in performance and usability. Mol Biol Evol 30:772–780. https://doi.org/10.1093/molbev/mst010.